Supporting information:

Identification of key regions mediating human melatonin type 1 receptor functional selectivity revealed by natural variants

Alan Hegron[1,2,3,14], Eunna Huh[4], Xavier Deupi[5,6], Badr Sokrat[2,3], Wenwen Gao[1], Christian Le Gouill[3], Mickaël Canouil[7,8,9], Mathilde Boissel[7,8,9], Guillaume Charpentier[10], Ronan Roussel[11], Beverley Balkau[12], Philippe Froguel[7,8,9], Bianca Plouffe[2,3,15], Amélie Bonnefond[7,8,9], Olivier Lichtarge[4,13], Ralf Jockers[1*], Michel Bouvier[2,3*]

Authors and affiliation.

[1]Université de Paris, Institut Cochin, CNRS, INSERM, F-75014 Paris, France

[2]Department of Biochemistry and Molecular Medicine, University de Montréal, Montreal, QC, Canada

[3]Institute for Research in Immunology and Cancer, University of Montreal, QC, Canada

[4]Department of Pharmacology, Baylor College of Medicine, Houston, TX 77030, United States of America

[5]Laboratory of Biomolecular Research, Paul Scherrer Institute (PSI), 5232 Villigen PSI, Switzerland

[6]Condensed Matter Theory group, Paul Scherrer Institute (PSI), 5232 Villigen PSI, Switzerland

[7]Inserm UMR1283, CNRS UMR8199, European Genomic Institute for Diabetes (EGID), Institut Pasteur de Lille, Lille, 59000, France;

[8]University of Lille, Lille University Hospital, Lille, 59000, France;

[9]Department of Metabolism, Imperial College London, London, W12 0NN, United Kingdom;

[10]CERITD (Centre d'Étude et de Recherche pour l'Intensification du Traitement du Diabète), Evry, France

[11]Department of Diabetology Endocrinology Nutrition, Hôpital Bichat, DHU FIRE, Assistance Publique Hôpitaux de Paris, Paris, France // Inserm U1138, Centre de Recherche des Cordeliers, Paris, France // UFR de Médecine, University Paris Diderot, Sorbonne Paris Cité, Paris, France

[12]Inserm U1018, Center for Research in Epidemiology and Population Health, Villejuif, France // University Paris-Saclay, University Paris-Sud, Villejuif, France

[13]Department of Molecular and Human Genetics, Baylor College of Medicine, Houston, TX 77030, United States of America

[14]Present address: Dept. of Molecular Pathobiology, New York University College of Dentistry, New York

[15]Present address: The Wellcome-Wolfson Institute for Experimental Medicine, Queen's University Belfast, Belfast, BT9 7BL, United Kingdom

***Corresponding authors:** Ralf Jockers, University of Paris, Institut Cochin, CNRS, INSERM, F-75014 Paris, France Email: ralf.jockers@inserm.fr and Michel Bouvier, University of Montreal, 2900 Boulevard Édouard-Montpetit, Montréal, Quebec, H3T 1J4, Canada, E-mail: michel.bouvier@umontreal.ca.

Table of contents:

Supporting Figures

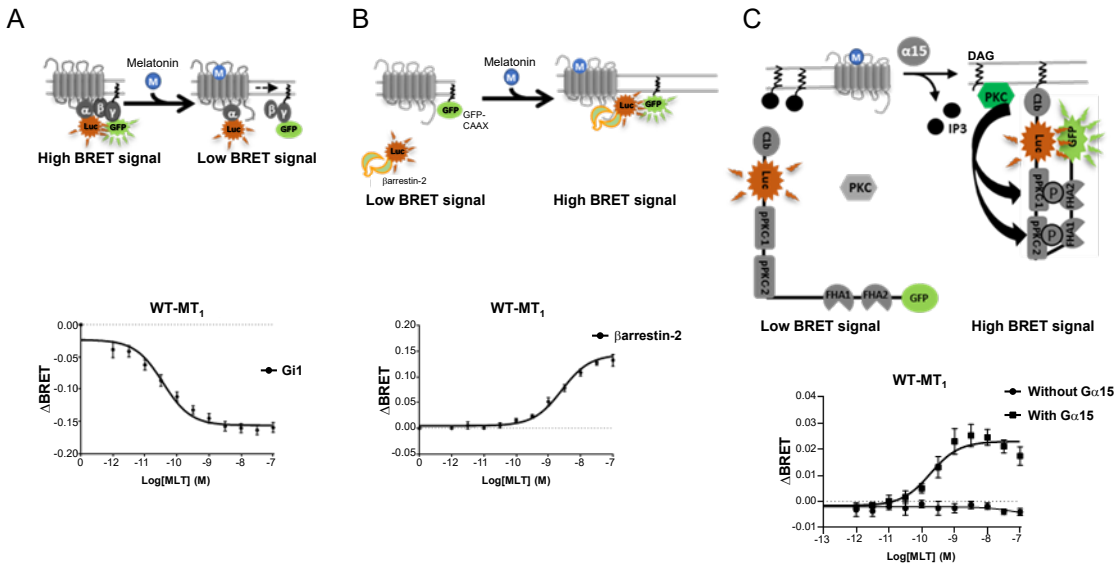

Figure S1. Representation of the different BRET-based biosensors used for MT1 characterization. (A) In basal condition, MT1 is bound to inactive complex αβγ (left part). In our case, we used α proteins fused to RlucII and Gγ proteins fused to GFP10. When melatonin is added, it binds to and activates the MT1 receptor leading to the dissociation of the complex (upper panel). RlucII too distant from GFP10 to transfer its energy, a decrease of BRET is observed (bottom panel). (B) For this experiment, we used βarrestin-2 fused to RlucII (βarrestin-2-RlucII) and the CAAX part of Kras protein which anchors to the plasma membrane fused to rGFP (CAAX-rGFP). In basal state, βarrestin-2 is not present at the plasma membrane (upper left panel). Upon MT1 activation by melatonin, βarrestin-2 is recruited to MT1 at the cell surface leading to a proximity between βarrestin-2-RlucII and CAAX-rGFP leading to an increase of EbBRET signal (upper right panel) as shown by the dose-response curve on the bottom panel. (C) The last BRET sensor used was the unimolecular biosensor of PKC activation. This biosensor contains the c1b domain of PKCδ able to bind DAG, RlucII, two specific phospho-substrate sequences (pPKC1 and pPKC2), two phospho-sensing domains (FHA1 and FHA2) and a rGFP (upper left panel). Upon MT1 activation by melatonin, Gα15 is activated leading to the activation of PLC, producing DAG and IP3 and PKC activation. This activated PKC and our biosensors are then able to bind to DAG present at the plasma membrane (upper right panel). PKC phosphorylates the biosensor, leading to its conformational change increasing the proximity of RlucII with rGFP and an increase of EbBRET (bottom panel).

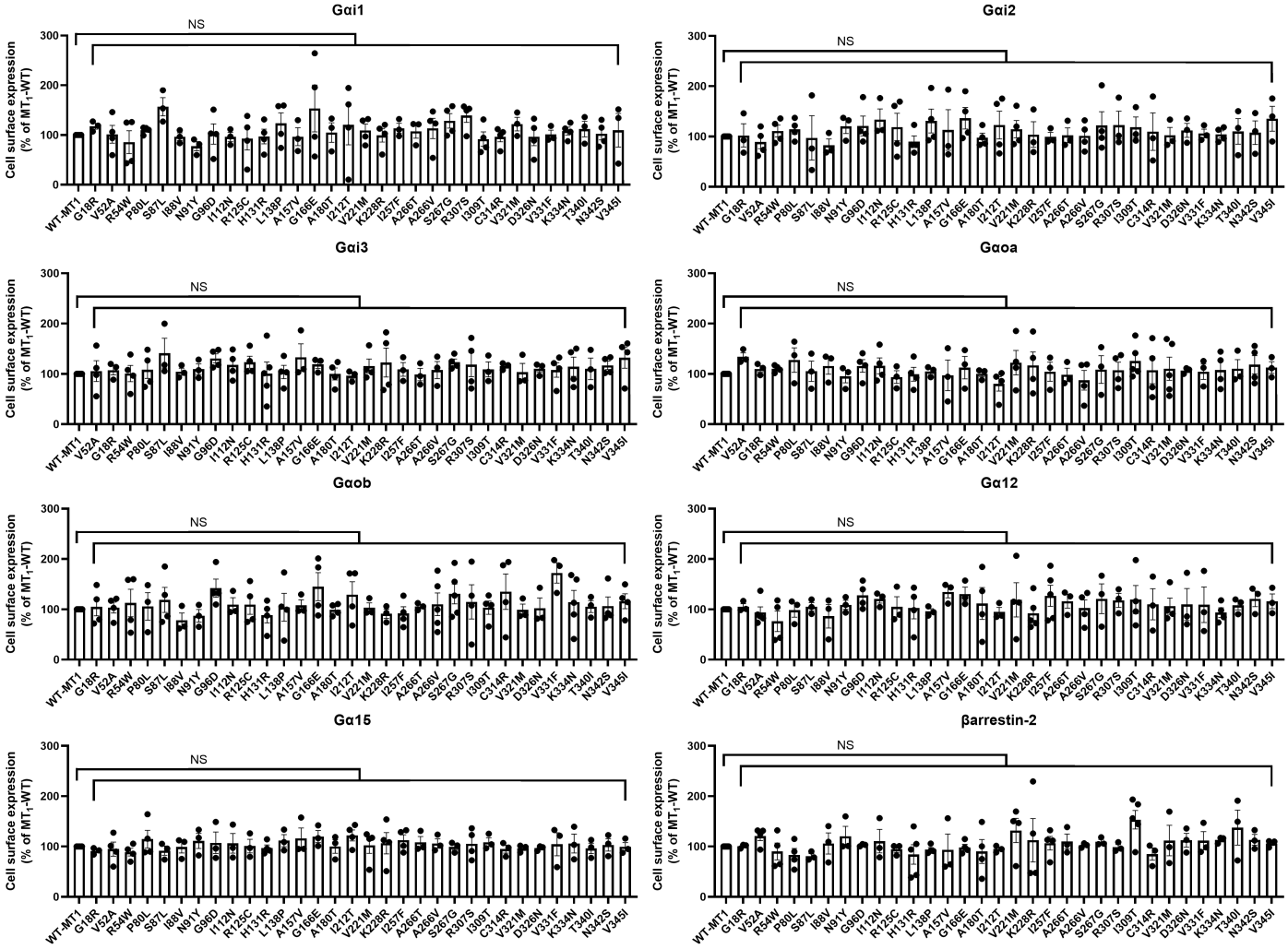

Figure S2. MT1 variant receptors are as expressed at the cell surface as the MT1-WT.
Cell surface expression of MT1 variants measured by enzyme-linked immunosorbent assay (ELISA) in HEK293 cells in parallel of BRET experiments for every G protein activation or βarrestin-2 recruitment. Cell surface expression of each variant was adjusted to MT1-WT. Statistical analysis was performed using one-sample t test. Data represents means ± SEM of 3 to 6 experiments. Data were fitted in GraphPad Prism 9.

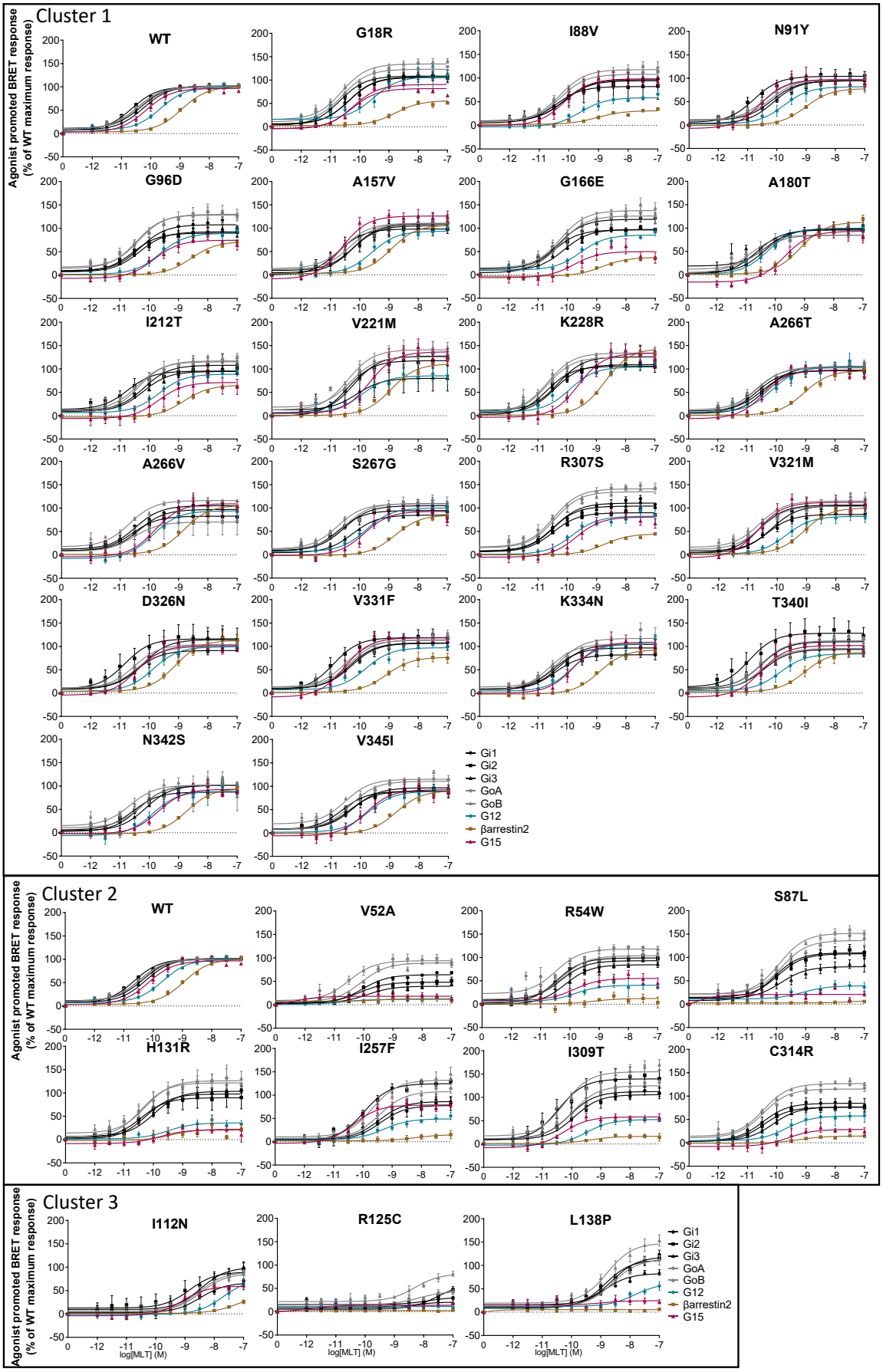
Cluster 1
Agonist promoted BRET response (% of WT maximum response)
WT
G18R
I88V
N91Y
G96D
A157V
G166E
A180T
I212T
V221M
K228R
A266T
A266V
S267G
R307S
V321M
D326N
V331F
K334N
T340I
N342S
V345I
Gi1
Gi2
Gi3
GoA
GoB
G12
βarrestin2
G15
Cluster 2
WT
V52A
R54W
S87L
H131R
I257F
I309T
C314R
Cluster 3
I112N
R125C
L138P
log[MLT] (M)

Figure S3. Melatonin concentration-response curves for G protein activation and βarrestin-2 recruitment of the MT_1-WT and the different variant profiles grouped in 3 clusters.

Functional profile of the MT_1-WT receptor and the first cluster corresponding to the 21 variants with a similar profile to the MT_1-WT receptor. The cluster 2 groups 7 variants with a total loss of βarrestin-2 recruitment and generally an impairment of Gα12 and/or Gα15 activation. The cluster 3 groups 3 variants with a loss of βarrestin-2 recruitment and a defect for every maximal efficacy (Max) but with similar potencies (EC50) to the MT_1-WT. Cell surface expression of each variant was adjusted to MT_1-WT and monitored by ELISA. Experiments were repeated at least 3 times. Data were plotted using non-linear regression with a fixed Hill slope equal to 1. Data points represent means ± SEM of 3 to 15 experiments. WT; wild-type. Data were fitted in GraphPad Prism 9.

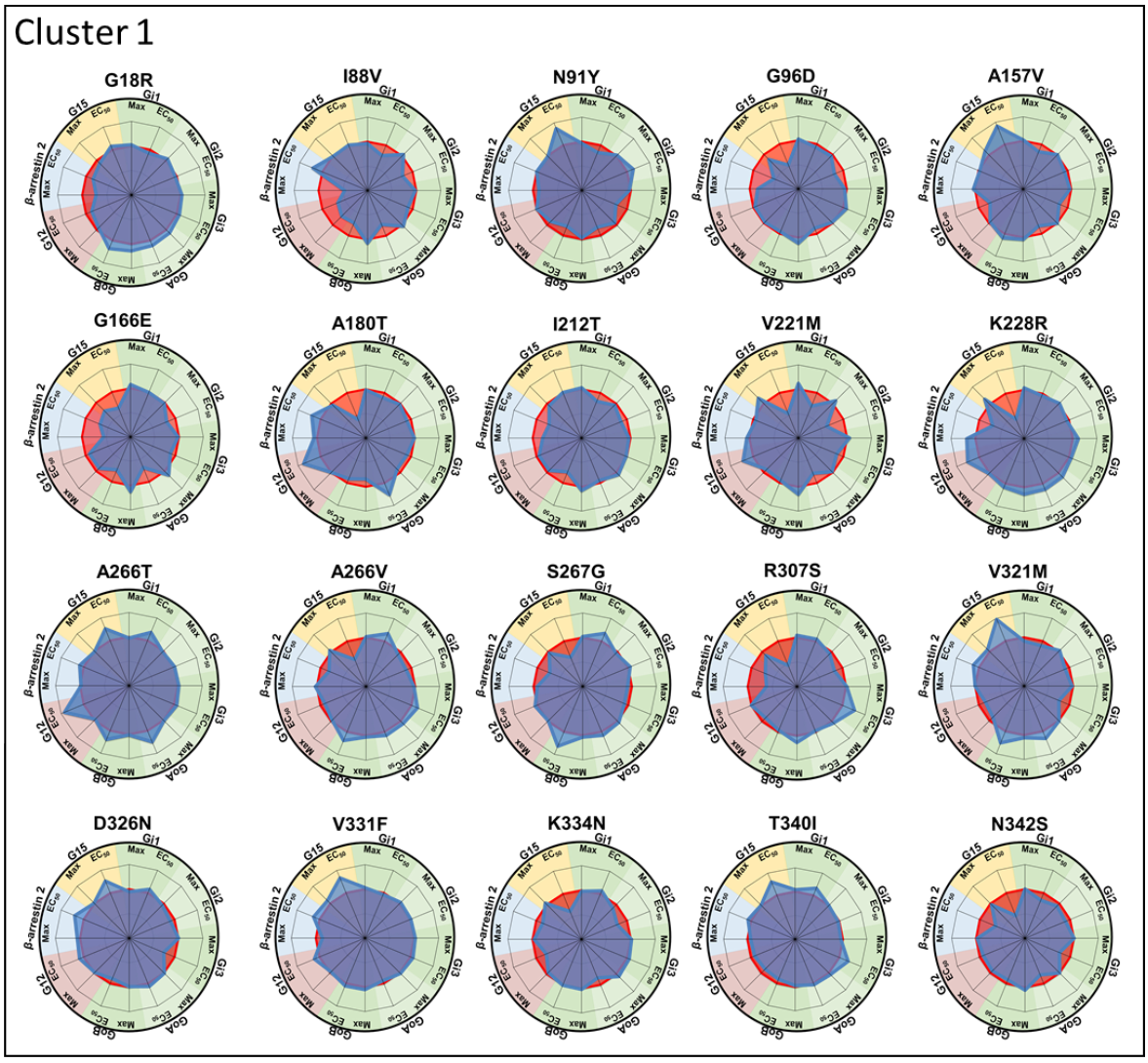
Cluster 1
G18R
I88V
N91Y
G96D
A157V
G166E
A180T
I212T
V221M
K228R
A266T
A266V
S267G
R307S
V321M
D326N
V331F
K334N
T340I
N342S

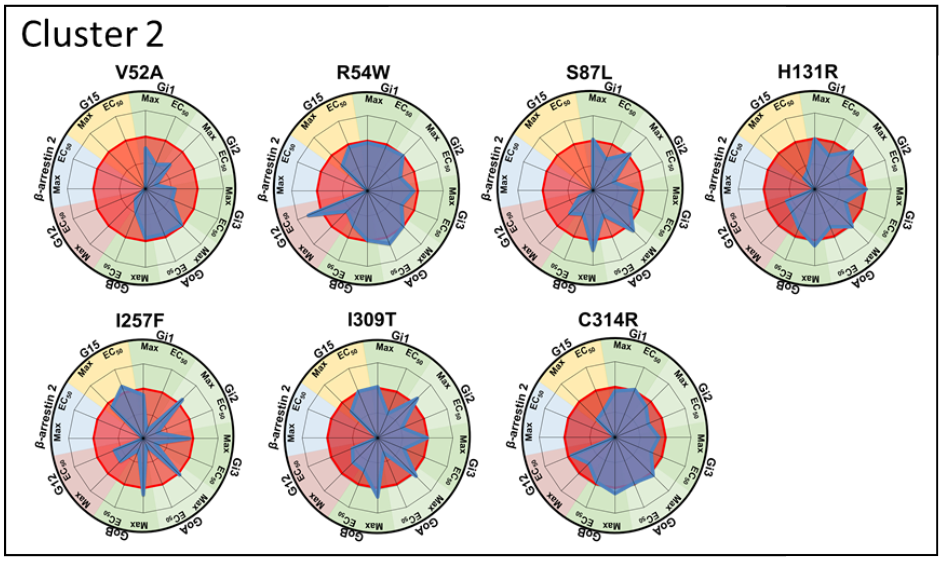
Cluster 2
V52A
R54W
S87L
H131R
I257F
I309T
C314R

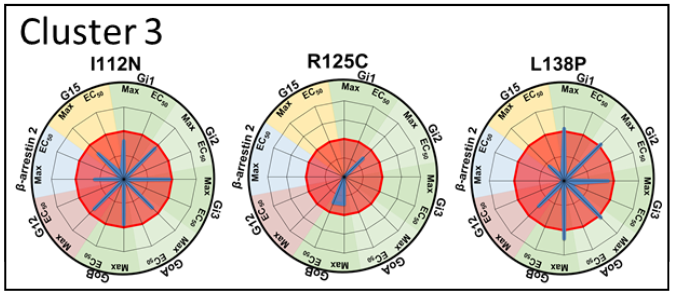
Cluster 3
I112N
R125C
L138P

Figure S4. Radial graph representation of the different variant profiles grouped in 3 clusters.
On each radial graph for each MT_1 variant, maximal agonist-induced efficacy (Max) and potency (EC50) obtained by BRET are indicated. The three clusters were made regarding the profile of each variant. The first cluster corresponds to the 21 variants with a similar profile to the MT_1-WT receptor. The cluster 2 groups 7 variants with a total loss of βarrestin-2 recruitment and generally an impairment of Gα activation potencies, especially for Gα12 and/or Gα15. The cluster 3 groups 3 variants with a defect for every efficacy (Max) but generally with similar potencies (EC50) to the MT_1-WT. WT profile is represented in red and mutant profiles are in blue. A loss of potency or efficacy for a specific protein results in the decrease of the blue area. Cell surface expression of each variant was adjusted to MT_1-WT and monitored by ELISA. Data were fitted in Microsoft Excel 2016.

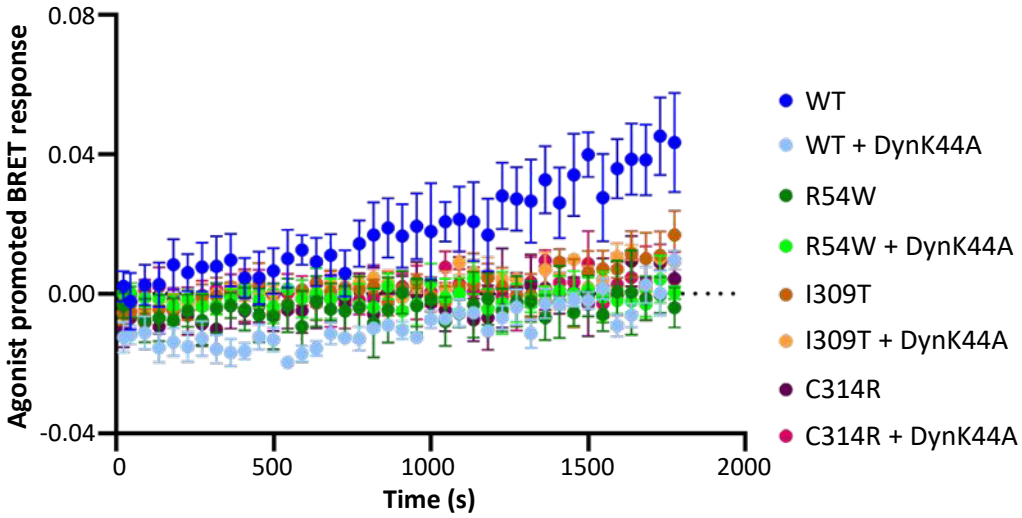

Figure S5. Kinetic of melatonin-induced MT1 internalization in response to melatonin.
Kinetic of melatonin-induced BRET response between MT1-WT (Blue), R54W (Green), I309T (Brown) and C314R (Purple) receptors fused to RlucII and the early endosome marker FYVE fused to rGFP, in absence (Dark curves) or presence (Clear curves) of the dominant negative Dynamin K44A (DynK44A) to inhibit endocytosis. Only MT1-WT receptor internalizes contrary to R54W, I309T and C314R. Data points represent means ± SEM of 3 experiments. WT; wild-type. Data were fitted in GraphPad Prism 9.

Supporting Tables

Table S1. Coding variants of *MTNR1A* (NM_005958.4) which were accurately detected in 8,687 individuals. 2,102 cases and 4,008 controls were involved in the case-control study for type 2 diabetes; 991 cases and 985 controls were involved in the case-control study for childhood obesity; 1,301 cases and 2,621 controls were involved in the case-control study for adulthood obesity.

Chr_Pos (hg19)	Ref	Mut	Conse-quence	AA change	GnomAD	Minor Allele Count					
						Type 2 diabetes		Obesity Childhood		Obesity Adulthood	
						Control	Case	Control	Case	Control	Case
4_187476468	C	T	NS	p.G18R	1	0	0	2	0	0	0
4_187476365	A	G	NS	p.V52A	1	3	0	3	1	1	1
4_187476360	G	A	NS	p.R54W	1	0	0	1	1	0	0
4_187476335	C	A	SD	p.?	1	0	1	0	0	0	0
4_187455657	G	A	NS	p.P80L	1	1	0	0	0	0	1
4_187455636	G	A	NS	p.S87L	1	0	1	0	0	0	0
4_187455634	T	C	NS	p.I88V	1	1	0	0	0	1	0
4_187455625	T	A	NS	p.N91Y	1	0	1	0	0	0	1
4_187455617	C	T	SG	p.W93*	1	1	0	0	0	1	0
4_187455609	C	T	NS	p.G96D	1	12	10	2	5	5	1
4_187455561	A	T	NS	p.I112N	0	0	1	0	0	0	1
4_187455523	G	A	NS	p.R125C	1	0	1	0	0	0	0
4_187455504	T	C	NS	p.H131R	1	1	0	1	0	0	1
4_187455483	A	G	NS	p.L138P	1	0	1	0	1	1	0
4_187455426	G	A	NS	p.A157V	1	0	1	0	0	0	0
4_187455399	C	T	NS	p.G166E	1	159	64	19	28	103	40
4_187455386	G	C	SG	p.Y170*	1	2	2	1	0	2	0
4_187455358	C	T	NS	p.A180T	1	1	1	0	0	2	0
4_187455261	A	G	NS	p.I212T	1	1	29	1	1	6	5
4_187455235	C	T	NS	p.V221M	1	0	0	0	1	0	1
4_187455213	T	C	NS	p.K228R	0	0	1	0	0	0	0
4_187455127	T	A	NS	p.I257F	1	1	0	0	0	1	0
4_187455100	C	T	NS	p.A266T	1	3	0	3	0	2	1
4_187455099	G	A	NS	p.A266V	1	152	93	42	26	102	49
4_187455097	T	C	NS	p.S267G	0	0	1	0	0	0	1
4_187454975	C	G	NS	p.R307S	0	1	0	1	0	0	0
4_187454956	A	G	NS	p.C314R	1	1	0	0	0	1	0
4_187454935	C	T	NS	p.V321M	1	1	1	0	0	0	0
4_187454920	C	T	NS	p.D326N	1	0	1	0	1	0	0
4_187454905	C	A	NS	p.V331F	1	0	1	0	0	0	0
4_187454894	T	A	NS	p.K334N	1	26	13	4	4	16	4
4_187454882	CAGTGGAGACGGTTTC	del	FS	p.W333*	1	1	1	0	0	2	0
4_187454877	G	A	NS	p.T340I	1	2	0	0	0	1	0
4_187454871	T	C	NS	p.N342S	0	1	0	0	0	0	0
4_187454863	C	T	NS	p.V345I	1	5	2	2	0	4	3
4_187454843	T	A	SL	p.*351Yext*?	0	1	0	0	0	0	0

AA, amino acid; Chr, chromosome; Del, deletion; FS, frameshift variant; GnomAD, genome aggregation database browser (v2.1.1; 1: present, 0: absent); Mut, mutated allele; NS, non-synonymous variant; Pos, position (according to the human alignment hg19/GRCh37); Ref, reference allele; SD, splice-donor variant; SG, stop-gain variant; SL, stop-loss variant.

Table S2. Association between *MTNR1A* coding variants and the risk of T2D, childhood obesity and adulthood obesity.

Study	Variant	OR [CI]	P_{π}	P_{τ}	*P*
CC T2D	Cluster of rare variants	1.17 [0.759-1.78]	0.473	0.373	0.483
CC ObC	Cluster of rare variants	0.669 [0.302-1.47]	0.315	0.464	0.427
CC ObA	Cluster of rare variants	0.706 [0.406-1.19]	0.201	0.383	0.275
CC T2D	p.G166E (rs28383653)	0.941 [0.676-1.30]	NA	NA	0.712
CC ObC	p.G166E (rs28383653)	2.28 [1.03-5.16]	NA	NA	0.0445
CC ObA	p.G166E (rs28383653)	0.804 [0.546-1.16]	NA	NA	0.257
CC T2D	p.A266V (rs28383652)	1.15 [0.855-1.54]	NA	NA	0.347
CC ObC	p.A266V (rs28383652)	0.757 [0.364-1.56]	NA	NA	0.451
CC ObA	p.A266V (rs28383652)	0.855 [0.596-1.21]	NA	NA	0.387

CC, case-control study; CI, confidence interval; NA, not applicable; ObC, obesity childhood; ObA, obesity adulthood; OR, odds ratio; π, mean effect of the cluster; τ, heterogeneous effect of the cluster

Table S3. Data from the functional characterization of variants. Summary of the functional profiling of (**A**) Gαi1, Gαi2, Gαi3, (**B**) GαoA, GαoB, (**C**) Gα12 and Gα15 activation and βarrestin-2 recruitment by MT_1-WT and MT_1 variants. Data represent the mean ± SEM of 3-13 independent experiments with repeats in quadruplicate. Data were analyzed by comparing independent fits.

A

	Gi1			Gi2			Gi3		
Receptor	Emax (% of WT)	LogEC50	Log(Tau/Ka)	Emax (% of WT)	LogEC50	Log(Tau/Ka)	Emax (% of WT)	LogEC50	Log(Tau/Ka)
WT-MT1		-10.54 ± 0.04	10.44 ± 0.05		-10.75 ± 0.03	10.64 ± 0.04		-10.4 ± 0.03	10.29 ± 0.03
G18R	104.9 ± 3.9	-10.47 ± 0.11	10.39 ± 0.08	108.3 ± 2.3	-10.72 ± 0.06	10.65 ± 0.07	106.1 ± 2.5	-10.45 ± 0.06	10.38 ± 0.06
I88V	92.9 ± 4.5	-10.34 ± 0.13	10.21 ± 0.09	108.7 ± 2.4	-10.55 ± 0.06	10.48 ± 0.08	95.67 ± 4.0	-10.31 ± 0.12	10.19 ± 0.07
N91Y	92.7 ± 2.7	-10.4 ± 0.085	10.27 ± 0.09	103.6 ± 3.3	-10.87 ± 0.09	10.78 ± 0.08	94.15 ± 2.6	-10.18 ± 0.07	10.05 ± 0.07
G96D	106.1 ± 3.3	-10.48 ± 0.09	10.4 ± 0.09	91.39 ± 2.9	-10.58 ± 0.09	10.43 ± 0.08	91.5 ± 3.1	-10.46 ± 0.10	10.33 ± 0.09
A157V	103.9 ± 5.0	-10.4 ± 0.14	10.32 ± 0.08	101.5 ± 3.6	-10.69 ± 0.10	10.6 ± 0.07	94.42 ± 2.0	-10.23 ± 0.05	10.11 ± 0.07
G166E	116.9 ± 3.8	-10.53 ± 0.09	10.49 ± 0.09	95.86 ± 1.7	-10.58 ± 0.05	10.46 ± 0.09	95.91 ± 2.4	-10.3 ± 0.07	10.19 ± 0.08
A180T	97.3 ± 3.4	-10.45 ± 0.10	10.34 ± 0.10	95.66 ± 2.0	-10.67 ± 0.06	10.55 ± 0.08	98.31 ± 2.3	-10.32 ± 0.07	10.21 ± 0.08
I212T	106.2 ± 4.9	-10.38 ± 0.13	10.3 ± 0.09	91.02 ± 2.2	-10.64 ± 0.07	10.5 ± 0.09	93.22 ± 2.2	-10.39 ± 0.06	10.26 ± 0.09
V221M	126.8 ± 2.5	-10.28 ± 0.05	10.28 ± 0.08	117.8 ± 4.8	-10.41 ± 0.11	10.38 ± 0.06	110.3 ± 4.8	-10.27 ± 0.12	10.22 ± 0.06
K228R	108.7 ± 2.7	-10.5 ± 0.07	10.44 ± 0.09	105.7 ± 4.0	-10.71 ± 0.11	10.64 ± 0.07	125.2 ± 4.0	-10.44 ± 0.09	10.44 ± 0.07
A266T	95.0 ± 4.3	-10.7 ± 0.13	10.57 ± 0.08	95.82 ± 2.6	-10.76 ± 0.08	10.64 ± 0.07	104.6 ± 2.9	-10.45 ± 0.08	10.37 ± 0.06
A266V	103.5 ± 2.2	-10.69 ± 0.06	10.6 ± 0.08	85.24 ± 3.4	-10.65 ± 0.12	10.48 ± 0.09	95.83 ± 2.8	-10.52 ± 0.08	10.41 ± 0.08
S267G	103.7 ± 2.9	-10.69 ± 0.08	10.6 ± 0.10	92.13 ± 1.9	-10.79 ± 0.06	10.66 ± 0.08	84.38 ± 2.0	-10.33 ± 0.06	10.16 ± 0.09
R307S	109.4 ± 2.7	-10.58 ± 0.07	10.51 ± 0.09	89.15 ± 1.7	-10.6 ± 0.05	10.45 ± 0.08	103.1 ± 2.7	-10.64 ± 0.07	10.56 ± 0.08
V321M	85.6 ± 3.0	-10.45 ± 0.10	10.28 ± 0.10	106 ± 4.2	-10.67 ± 0.11	10.59 ± 0.08	96.09 ± 2.3	-10.2 ± 0.06	10.09 ± 0.08
D326N	90.0 ± 2.7	-10.61 ± 0.09	10.46 ± 0.10	90.44 ± 1.5	-10.67 ± 0.05	10.53 ± 0.1	101.1 ± 2.5	-10.19 ± 0.06	10.1 ± 0.08
V331F	105.9 ± 3.6	-10.51 ± 0.10	10.43 ± 0.08	105.8 ± 1.5	-10.76 ± 0.04	10.68 ± 0.08	105.3 ± 3.1	-10.45 ± 0.08	10.37 ± 0.06
K334N	95.7 ± 2.3	-10.6 ± 0.07	10.48 ± 0.09	81.25 ± 3.3	-10.56 ± 0.12	10.37 ± 0.11	103 ± 2.5	-10.44 ± 0.07	10.35 ± 0.08
T340I	108.5 ± 2.5	-10.68 ± 0.07	10.61 ± 0.08	100.3 ± 2.3	-10.73 ± 0.06	10.63 ± 0.09	92.25 ± 3.8	-10.58 ± 0.12	10.44 ± 0.07
N342S	100.9 ± 3.4	-10.4 ± 0.09	10.3 ± 0.10	86.42 ± 2.2	-10.66 ± 0.07	10.49 ± 0.10	100.8 ± 2.1	-10.19 ± 0.05	10.1 ± 0.08
V345I	88.5 ± 4.0	-10.53 ± 0.13	10.37 ± 0.10	88.46 ± 2.1	-10.77 ± 0.07	10.62 ± 0.08	95.68 ± 1.9	-10.39 ± 0.05	10.27 ± 0.08
V52A	64.0 ± 1.7	-10.07 ± 0.07	9.77 ± 0.16	49.33 ± 4.2	-9.81 ± 0.22	9.401 ± 0.16	39.25 ± 1.7	-9.98 ± 0.12	9.47 ± 0.18
R54W	91.8 ± 3.0	-10.49 ± 0.09	10.35 ± 0.11	98.79 ± 3.9	-10.48 ± 0.11	10.38 ± 0.08	84.44 ± 3.0	-10.16 ± 0.10	9.99 ± 0.10
S87L	104.9 ± 3.4	-10.25 ± 0.09	10.17 ± 0.1	108.7 ± 4.0	-10.2 ± 0.10	10.13 ± 0.08	77.33 ± 4.1	-10.22 ± 0.14	10.01 ± 0.10
H131R	97.6 ± 2.6	-10.29 ± 0.07	10.17 ± 0.10	111.6 ± 3.1	-10.47 ± 0.08	10.42 ± 0.07	102.5 ± 3.1	-10.09 ± 0.08	10.01 ± 0.08
I257F	77.2 ± 5.1	-9.482 ± 0.16	9.26 ± 0.12	124.3 ± 3.1	-9.998 ± 0.06	9.991 ± 0.07	85.21 ± 3.7	-9.57 ± 0.10	9.40 ± 0.08
I309T	104.1 ± 2.8	-10.09 ± 0.07	10 ± 0.08	126.5 ± 2.8	-10.3 ± 0.06	10.3 ± 0.07	97.78 ± 2.5	-9.99 ± 0.06	9.88 ± 0.08
C314R	84.2 ± 4.1	-10.56 ± 0.14	10.38 ± 0.12	75.89 ± 2.8	-10.49 ± 0.10	10.27 ± 0.11	76.46 ± 1.7	-10.2 ± 0.06	9.98 ± 0.10
I112N	65.8 ± 5.6	-8.555 ± 0.16	8.27 ± 0.15	83.08 ± 3.2	-8.71 ± 0.07	8.528 ± 0.11	89.65 ± 3.2	-8.49 ± 0.06	8.34 ± 0.08
R125C	NR	NR	NR	53.06 ± 6.8	-7.798 ± 0.17	7.42 ± 0.22	NR	NR	NR
L138P	111.7 ± 6.5	-8.948 ± 0.12	8.89 ± 0.1	109.1 ± 4.0	-9.015 ± 0.07	8.951 ± 0.08	78.62 ± 3.7	-9.23 ± 0.11	9.03 ± 0.11
P80L	NR	NR	NR	NR	NR	NR	NR	NR	NR

B

Receptor	GoA			GoB		
	Emax (% of WT)	LogEC50	Log(Tau/Ka)	Emax (% of WT)	LogEC50	Log(Tau/Ka)
WT-MT1		-10.65 ± 0.04	10.53 ± 0.04		-10.68 ± 0.04	10.5 ± 0.05
G18R	121.9 ± 2.1	-10.75 ± 0.05	10.71 ± 0.07	132.4 ± 2.8	-10.84 ± 0.06	10.79 ± 0.06
I88V	106.8 ± 3.0	-10.43 ± 0.08	10.34 ± 0.08	116.7 ± 3.3	-10.43 ± 0.08	10.33 ± 0.07
N91Y	89.74 ± 2.1	-10.49 ± 0.06	10.33 ± 0.12	94.97 ± 2.5	-10.5 ± 0.07	10.31 ± 0.09
G96D	95.62 ± 5.7	-10.54 ± 0.17	10.4 ± 0.11	126.5 ± 2.9	-10.64 ± 0.06	10.58 ± 0.08
A157V	99.66 ± 2.1	-10.5 ± 0.06	10.38 ± 0.10	108.5 ± 2.6	-10.76 ± 0.07	10.62 ± 0.08
G166E	124.9 ± 4.8	-10.36 ± 0.11	10.34 ± 0.08	128.7 ± 4.2	-10.44 ± 0.09	10.38 ± 0.07
A180T	82.55 ± 2.6	-10.88 ± 0.11	10.68 ± 0.14	72.56 ± 1.9	-10.6 ± 0.08	10.29 ± 0.15
I212T	113.7 ± 4.8	-10.6 ± 0.12	10.54 ± 0.09	116.3 ± 2.8	-10.46 ± 0.06	10.35 ± 0.09
V221M	95.85 ± 5.8	-10.46 ± 0.18	10.33 ± 0.11	136.7 ± 3.9	-10.63 ± 0.09	10.6 ± 0.07
K228R	124.4 ± 3.0	-10.76 ± 0.08	10.73 ± 0.09	133.5 ± 3.7	-10.75 ± 0.09	10.71 ± 0.08
A266T	102.7 ± 2.8	-10.87 ± 0.08	10.77 ± 0.08	101.5 ± 1.9	-10.85 ± 0.05	10.69 ± 0.08
A266V	115.3 ± 3.0	-10.72 ± 0.08	10.67 ± 0.09	106.8 ± 3.5	-10.85 ± 0.10	10.71 ± 0.08
S267G	108.1 ± 3.6	-10.72 ± 0.10	10.64 ± 0.10	107.3 ± 2.4	-10.97 ± 0.07	10.83 ± 0.09
R307S	111.5 ± 3.8	-10.63 ± 0.18	10.56 ± 0.09	132.8 ± 3.2	-10.65 ± 0.07	10.6 ± 0.07
V321M	102 ± 2.4	-10.79 ± 0.07	10.69 ± 0.09	112.6 ± 3.0	-10.91 ± 0.08	10.79 ± 0.08
D326N	102.5 ± 2.9	-10.71 ± 0.08	10.6 ± 0.09	97.87 ± 2.6	-10.59 ± 0.07	10.41 ± 0.09
V331F	104.6 ± 2.6	-10.6 ± 0.07	10.5 ± 0.10	110.9 ± 3.2	-10.73 ± 0.08	10.61 ± 0.08
K334N	115 ± 4.2	-10.52 ± 0.10	10.46 ± 0.09	104.2 ± 2.0	-10.69 ± 0.05	10.54 ± 0.08
T340I	110.6 ± 2.8	-10.68 ± 0.07	10.61 ± 0.08	94.81 ± 2.6	-10.6 ± 0.08	10.41 ± 0.09
N342S	100.9 ± 2.7	-10.48 ± 0.07	10.36 ± 0.10	112.4 ± 3.7	-10.61 ± 0.09	10.5 ± 0.08
V345I	109.3 ± 2.5	-10.47 ± 0.06	10.39 ± 0.09	112.4 ± 2.9	-10.85 ± 0.08	10.15 ± 0.07
V52A	93.59 ± 3.2	-10.59 ± 0.10	10.45 ± 0.09	88.61 ± 2.4	-10.18 ± 0.07	9.95 ± 0.10
R54W	98.04 ± 6.2	-10.77 ± 0.20	10.65 ± 0.10	96.33 ± 4.3	-10.45 ± 0.13	10.27 ± 0.09
S87L	131.2 ± 4.4	-10.21 ± 0.09	10.21 ± 0.08	147.3 ± 4.6	-10.22 ± 0.08	10.22 ± 0.07
H131R	108.2 ± 5.8	-10.47 ± 0.16	10.39 ± 0.09	124.4 ± 5.0	-10.52 ± 0.12	10.45 ± 0.07
I257F	105.9 ± 4.1	-9.58 ± 0.09	9.48 ± 0.09	130.1 ± 4.4	-9.83 ± 0.09	9.78 ± 0.07
I309T	118.6 ± 2.6	-9.92 ± 0.05	9.88 ± 0.09	143.3 ± 3.8	-10.42 ± 0.07	10.41 ± 0.07
C314R	113.8 ± 2.1	-10.63 ± 0.05	10.57 ± 0.09	125.3 ± 3.0	-10.64 ± 0.07	10.57 ± 0.08
I112N	71.23 ± 4.5	-8.34 ± 0.11	8.08 ± 0.14	87.96 ± 3.5	-8.63 ± 0.07	8.41 ± 0.11
R125C	NR	NR	NR	55.41 ± 4.5	-10.44 ± 0.23	10 ± 0.18
L138P	109.2 ± 5.5	-8.82 ± 0.10	8.74 ± 0.10	140 ± 7.2	-9.12 ± 0.11	9.10 ± 0.07
P80L	NR	NR	NR	NR	NR	NR

C

Receptor	G12			βarrestin-2			G15		
	Emax (% of WT)	LogEC50	Log(Tau/Ka)	Emax (% of WT)	LogEC50	Log(Tau/Ka)	Emax (% of WT)	LogEC50	Log(Tau/Ka)
WT-MT1		-9.84 ± 0.04	9.82 ± 0.04		-9 ± 0.03	8.88 ± 0.02		-9.14 ± 0.05	8.99 ± 0.06
G18R	89.46 ± 5.6	-9.73 ± 0.16	9.67 ± 0.11	55.8 ± 1.9	-8.86 ± 0.09	8.53 ± 0.10	83.5 ± 2.0	-9.20 ± 0.06	8.99 ± 0.11
I88V	58.97 ± 2.8	-9.53 ± 0.11	9.29 ± 0.15	30.39 ± 1.7	-9.18 ± 0.12	8.53 ± 0.19	98.43 ± 5.1	-9.15 ± 0.14	9.01 ± 0.11
N91Y	82.38 ± 4.2	-9.84 ± 0.13	9.74 ± 0.09	78.17 ± 2.1	-9.00 ± 0.05	8.76 ± 0.07	97.41 ± 4.6	-9.48 ± 0.13	9.33 ± 0.12
G96D	94.22 ± 2.8	-9.81 ± 0.07	9.77 ± 0.10	71.62 ± 1.7	-8.57 ± 0.05	8.35 ± 0.07	75.22 ± 4.2	-8.70 ± 0.14	8.44 ± 0.14
A157V	93.69 ± 3.4	-9.61 ± 0.09	9.57 ± 0.09	106.2 ± 2.1	-8.98 ± 0.04	8.87 ± 0.05	126.5 ± 4.0	-9.52 ± 0.09	9.49 ± 0.09
G166E	83.89 ± 3.3	-9.76 ± 0.10	9.68 ± 0.10	37.96 ± 1.2	-8.71 ± 0.07	8.21 ± 0.13	60.05 ± 3.3	-8.82 ± 0.14	8.46 ± 0.20
A180T	99.08 ± 2.2	-10.19 ± 0.06	10.17 ± 0.09	112.6 ± 3.6	-9.17 ± 0.07	9.13 ± 0.05	90.96 ± 5.8	-8.55 ± 0.15	8.37 ± 0.11
I212T	87.93 ± 3.4	-9.79 ± 0.10	9.72 ± 0.10	65.79 ± 1.8	-8.74 ± 0.07	8.48 ± 0.07	88.05 ± 4.1	-9.15 ± 0.12	8.96 ± 0.13
V221M	84.5 ± 4.9	-10.04 ± 0.15	9.96 ± 0.12	110.9 ± 2.5	-8.94 ± 0.05	8.84 ± 0.05	136.2 ± 6.7	-8.71 ± 0.12	8.71 ± 0.08
K228R	102.7 ± 4.0	-10.07 ± 0.10	10.07 ± 0.10	143.5 ± 4.8	-8.72 ± 0.07	8.80 ± 0.05	134.2 ± 6.4	-8.58 ± 0.12	8.57 ± 0.07
A266T	94.77 ± 5.3	-10.24 ± 0.15	10.21 ± 0.09	96.25 ± 2.4	-9.07 ± 0.06	8.94 ± 0.05	97.98 ± 2.4	-9.37 ± 0.07	9.23 ± 0.09
A266V	94.74 ± 2.9	-9.76 ± 0.08	9.72 ± 0.09	105.9 ± 1.9	-8.83 ± 0.04	8.78 ± 0.04	109.6 ± 5.4	-8.77 ± 0.12	8.67 ± 0.09
S267G	98.97 ± 3.8	-9.89 ± 0.10	9.87 ± 0.09	85.42 ± 1.8	-8.75 ± 0.05	8.59 ± 0.05	93.02 ± 4.7	-8.82 ± 0.13	8.65 ± 0.11
R307S	82.27 ± 3.5	-9.84 ± 0.11	9.75 ± 0.10	44.72 ± 1.0	-8.72 ± 0.05	8.31 ± 0.11	80.99 ± 5.2	-8.62 ± 0.16	8.4 ± 0.13
V321M	82.19 ± 4.2	-9.72 ± 0.13	9.62 ± 0.10	99.99 ± 2.6	-9.10 ± 0.08	8.97 ± 0.06	112.4 ± 3.8	-9.59 ± 0.10	9.51 ± 0.10
D326N	98.68 ± 3.2	-9.92 ± 0.08	9.90 ± 0.09	112.5 ± 4.0	-9.17 ± 0.08	9.09 ± 0.05	101.9 ± 3.3	-9.37 ± 0.09	9.25 ± 0.11
V331F	95.75 ± 2.8	-9.94 ± 0.07	9.91 ± 0.09	76.52 ± 3.9	-9.11 ± 0.11	8.87 ± 0.07	118.6 ± 3.3	-9.44 ± 0.08	9.38 ± 0.09
K334N	91.81 ± 3.7	-9.65 ± 0.10	9.60 ± 0.09	93.33 ± 1.8	-8.87 ± 0.05	8.75 ± 0.05	109 ± 5.5	-8.79 ± 0.13	8.69 ± 0.09
T340I	80.05 ± 4.5	-9.77 ± 0.14	9.66 ± 0.12	87.13 ± 4.0	-9.06 ± 0.10	8.87 ± 0.07	102.1 ± 4.9	-9.417± 0.13	9.29 ± 0.11
N342S	89.22 ± 5.6	-9.77 ± 0.16	9.71 ± 0.10	95.11 ± 1.8	-8.68 ± 0.04	8.55 ± 0.05	93.31 ± 3.6	-8.66 ± 0.09	8.49 ± 0.11
V345I	93.51 ± 3.1	-9.7 ± 0.08	9.65 ± 0.09	90.83 ± 2.0	-8.74 ± 0.05	8.62 ± 0.05	93.19 ± 5.7	-8.72 ± 0.15	8.56 ± 0.11
V52A	15.86 ± 5.9	-7.95 ± 0.54	7.14 ± 0.78	NR	NR	NR	NR	NR	NR
R54W	39.75 ± 4.0	-10.08 ± 0.27	9.66 ± 0.25	NR	NR	NR	54.33 ± 4.0	-9.09 ± 0.20	8.69 ± 0.20
S87L	48.06 ± 4.1	-9.06 ± 0.18	8.73 ± 0.22	NR	NR	NR	NR	NR	NR
H131R	45.54 ± 3.8	-9.47 ± 0.20	9.12 ± 0.22	NR	NR	NR	17.84 ± 3.6	-8.50 ± 0.49	7.61 ± 0.58
I257F	47.84 ± 3.6	-9.50 ± 0.18	9.17 ± 0.21	NR	NR	NR	79.14 ± 3.0	-9.25 ± 0.10	9.02 ± 0.14
I309T	52.89 ± 2.9	-9.41 ± 0.13	9.13 ± 0.17	NR	NR	NR	58.42 ± 3.1	-9.14 ± 0.13	8.78 ± 0.20
C314R	57.12 ± 4.9	-9.78 ± 0.22	9.52 ± 0.15	NR	NR	NR	33.11 ± 2.9	-8.75 ± 0.23	8.13 ± 0.36
I112N	75.89 ± 12.5	-7.66 ± 0.20	7.53 ± 0.15	43.35 ± 8.3	-7.27 ± 0.18	6.78 ± 0.21	60.19 ± 3.3	-8.00 ± 0.12	7.65 ± 0.21
R125C	NR	NR	NR	NR	NR	NR	NR	NR	NR
L138P	56.13 ± 7.3	-8.26 ± 0.22	7.99 ± 0.17	NR	NR	NR	26.54 ± 5.1	-7.89 ± 0.40	7.17 ± 0.46
P80L	NR	NR	NR	NR	NR	NR	NR	NR	NR

NR denotes that the experimental parameter could not be determined due to lack of a concentration-response curve.